Clin. Lab. 2024;70:XXX-XXX

ORIGINAL ARTICLE

The Protein S Erlangen Mutation *PROS1*$_{c.1904T>C}$ (F635S) Suppresses Secretion

Julian Reißig, Sarah Cunningham, Alexandra Wandersee, Regine Brox, Susanne Achenbach, Julian Strobel, Holger Hackstein, Sabine Schneider

Department of Transfusion Medicine and Hemostaseology, Friedrich-Alexander-University Erlangen-Nürnberg (FAU), University Hospital Erlangen, Erlangen, Germany

SUMMARY

Background: **The recently identified *PROS1* mutation Protein S Erlangen c.1904T>C, resulting in amino acid exchange F635S, is associated with severe quantitative protein S (PS) deficiency and clinical thrombosis. It was hypothesized that this deficiency is due to a secretion defect [1]. This report aims to further elucidate the potential secretion defect of PS Erlangen.**
Methods: **Coding sequences (CDS) of wild type (WT) *PROS1* (encoding PS) and mutated *PROS1*$_{c.1904T>C}$ (encoding PS$_{F635S}$) were cloned in front of the CDS of green fluorescent protein (GFP), and the respective plasmids were introduced into HEK293T cells. *PROS1-GFP* and *PROS1*$_{c.1904T>C}$*-GFP* expressing HEK293T cell lines were analyzed by confocal laser scanning microscopy and western blot for cellular proteins and proteins secreted to the growth medium.**
Results: **Western blot analysis revealed a significantly reduced secretion of PS$_{F635S}$ compared to WT PS. This observation was confirmed by the detection of mutant PS$_{F635S}$-GFP fusion exclusively in the endoplasmic reticulum (ER), while PS-GFP passed through the entire secretory pathway, as indicated by the localization within both the ER and Golgi apparatus.**
Conclusions: **The Protein S Erlangen mutation results in type I PS deficiency caused by a secretion defect.**
(Clin. Lab. 2024;70:xx-xx. DOI: 10.7754/Clin.Lab.2023.230906)

Correspondence:
Sabine Schneider
Department of Transfusion Medicine and Hemostaseology
University Hospital of Erlangen
Krankenhausstr. 12
91054 Erlangen
Germany
Phone: +49 9131-8536404
FAX: +49 9131-8536973
Email: sabine.schneider@uk-erlangen.de

Manuscript accepted September 14, 2023

KEYWORDS

Protein S deficiency, *PROS1*, point mutation, secretion defect, secretion pathway

INTRODUCTION

We have recently identified a novel Protein S (PS) mutation associated with clinically relevant thrombosis [1]. PS, a vitamin K-dependent plasma protein, is vital for the degradation of activated factor V and activated factor VIII by acting as a non-catalytic cofactor of activated protein C [2,3]. The mature PS antigen is composed of an N-terminal γ-carboxyglutamic acid-rich (Gla) domain, a thrombin-sensitive region, four epidermal growth factor (EGF)-like domains, and a large C-terminal sex-hormone binding globulin (SHBG)-like domain, consisting of Laminin G (LG)-like domain LG1

and LG2 [4].
PS is primarily produced in and secreted by hepatocytes and liver endothelial cells while also being present in plasma as a free antigen in its active form (~40%), or bound to C4b-binding protein in its inactive form (~60%) [5,6].
PS deficiency is classified into three categories: type I with a reduction in total PS and free PS resulting in reduced PS activity (quantitative defect); type II with total and free PS within normal range, but reduced PS activity (qualitative defect); and type III with decreased PS activity and decreased free PS, but normal total PS levels [7].
Type I deficiency can be caused by gross deletions [8], mutations that result in premature stop codons [9-13], defective splicing [11,14-16], reduced mRNA translation [17] or by a defective secretion based on missense mutations that inhibit a correct folding [10,11,13,18,19].
We postulated a secretion defect for PS with the Erlangen mutation according to the fact that several C-terminal mutations proximal to F635S were shown to result in a secretion defect [1,10,12,18-20]. Nevertheless, we could not completely exclude possible other factors as, for example, a reduced translation rate at that time point. Here, we show that PS deficiency caused by the PS Erlangen mutation (c.1904T>C; F635S) is due to a secretion defect using a HEK293T expression system.

MATERIALS AND METHODS

Construct generation

Plasmids for expressing a C-terminal *GFP* fusion of WT *PROS1* (referring to transcript NM_000313.4) or *PROS1*$_{c.1904T>C}$ CDS were produced by polymerase chain reaction (PCR) and ligated by Gibson assembly [21] using pcDNA3.1(+)/Puro/FA/GFP-LL5BIP as the expression vector [kindly provided from Tomasz Proszyski (Addgene plasmid #112829; http://n2t.net/addgene:112829; RRID:Addgene_112829)]. A four amino acid linker (GGSG) was inserted in front of the GFP. NEBuilder Assembly Tool (https://nebuilder.neb.com/#!/) was used to design PCR primers with overlapping sequences between the adjacent DNA fragments and for the assembly into the cloning vector according to the manufacturer's instructions (Gibson Assembly® Master Mix/Gibson Assembly® Cloning Kit NEB, New England Biolabs, Ipswich, MA, USA). Oligonucleotides were obtained from Merck, Darmstadt, Germany.
Insert sequences and vector fragments with complementary overhangs were amplified by PCR using the following primers (and templates):
PROS1 WT CDS fragment: PROS1_fwd
(5'-GTACCGAGCTCGGATCCATGAGGGTCCTGGGTGGGC-3')
and PROS1_rev
(5'-CATACCGCTACCGCCAGAATTCTTTGTCTTTTTCCAAACTGATGGACATGAGTGAG-3')
(*PROS1* WT cDNA from a healthy donor with informed consent, ethics committee vote #357_19 B, #343_18 B)
GFP CDS fragment:
GFP_fwd
(5'-GAATTCTGGCGGTAGCGGTATGGTGAGCAAGGGCGAGGAG-3')
and GFP_rev
(5'-GCACAGTCGAGGCTGATCACTTGTACAGCTCGTCCATGCCG-3')
(pcDNA3.1(+)/Puro/FA/GFP-LL5BIP)
vector pcDNA3.1 fragment: pcDNA3.1_fwd
(5'-GGACGAGCTGTACAAGTGATCAGCCTCGACTGTGCCTTCTAG-3')
and pcDNA3.1_rev
(5'-GACCCTCATGGATCCGAGCTCGGTACCAAG-3')
(pcDNA3.1(+)/Puro/FA/GFP-LL5BIP).
The PCR products were combined via Gibson assembly using the Gibson Assembly Master Mix (New England Biolabs, Ipswich, MA, USA) in accordance with the manufacturer's instructions yielding plasmid pJR01.
The *PROS1* c.1904T>C point mutation was generated by site-directed mutagenesis [22] with custom synthesized primers (Merck, Darmstadt, Germany) using the Q5 Site-Directed Mutagenesis Kit (New England Biolabs, Ipswich, MA, USA) with plasmid pJR01 as the template and oligonucleotides
M1-pBWCS1_F635S_fwd
(5'-GAATGCCTCTTATAATGGCTGCATGGAAGTG-3')
and M1-pBWCS1_F635S_rev
(5'-GCAGCCATTATAAGAGGCATTCACTGGTGTG-3').
The amplification conditions were 10 seconds at 98°C, 15 seconds at 68°C, and 3 minutes at 72°C for 30 cycles.
The PCR mixture was subsequently treated with 0.7 µL DpnI (New England Biolabs, Ipswich, MA, USA) and incubated for 3 hours at 37°C to digest the methylated parental DNA template. The target construct (pJR02) consisted of non-methylated DNA and is thus resistant to DpnI digestion. Nick repair of the mutated plasmid was conducted by transformation into NEB® 5-alpha Competent *E. coli* (New England Biolabs, Ipswich, MA, USA) in accordance to the manufacturer`s instructions.
The sequence integrity of all constructs was confirmed by Sanger Sequencing using the Mix2Seq Kit (Eurofins Genomics, Ebersberg, Germany).

Transfection and cell culture

HEK293T cells (ACC 635, DSMZ, Braunschweig, Germany) were grown in DMEM (#D6429, Sigma-Aldrich, Taufkirchen, Germany) supplemented with 10% FCS (anprotec, Bruckberg, Germany), 1% GlutaMAX (Thermo Fisher Scientific, Waltham, MA, USA), 1% Penicillin-Streptomycin (Sigma-Aldrich, Taufkirchen, Germany) at 37°C and 5% CO_2 in a humidified incubator. HEK293T cells were transiently transfected with pJR01

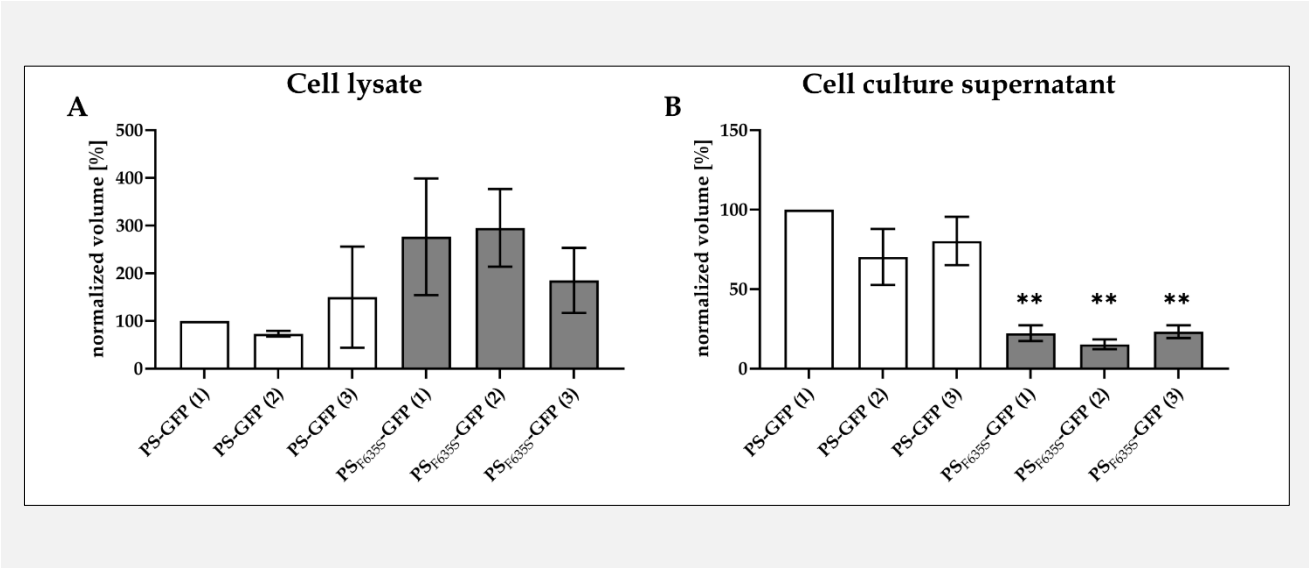

Figure 1. Protein S Erlangen mutation causes a secretion defect.

Western blot data from HEK293T cell lines expressing *PROS1-GFP* (PS-GFP) or *PROS1*$_{c.1904T>C}$*-GFP* (PS$_{F635S}$-GFP) (three independent lines per construct were analyzed; number of technical replicates per cell line = 3). GFP fusion protein amount was determined within cells (A) and in the growth medium (B), with a highly significant reduction in secretion of PS$_{F635S}$-GFP. Asterisks indicate a significant difference ($p < 0.01$) of PS$_{F635S}$-GFP lines compared to each PS-GFP line, error bars indicate standard deviation. Amounts of GFP fusion proteins were normalized to GFP fusion amount of PS-GFP (1), which was set as 100%.

or pJR02 via *Trans*IT®-293 Transfection Reagent (Mirus Bio LLC, Madison, WI, USA) according to the manufacturer's instructions. The medium was replaced after 24 hours with fresh medium containing 5 µg/mL Puromycin (Carl Roth, Karlsruhe, Germany) to select the transfected cells. Clones were picked after 1 - 2 weeks and analyzed by flow cytometry (CytoFLEX S, Beckman Coulter, Brea, CA, USA) for *GFP* expression.

Cell preparation and western blot

About 2 x 10^6/mL – 1 x 10^7/mL cells per cell line were cultivated in 1 mL EX-CELL® 293 serum-free culture medium (Sigma-Aldrich, Taufkirchen, Germany) for 48 hours at 37°C without antibiotics, followed by centrifugation at 300 x g at 4°C for 10 minutes. Supernatants were gently removed, transferred to a fresh tube and supplemented with cOmplete™ Mini protease inhibitor (Sigma-Aldrich, Taufkirchen, Germany). The remaining cell pellets were resuspended in 300 µL RIPA buffer (50 mM Tris-HCl, pH 8.0, 150 mM NaCl, 0.5% sodium deoxycholate, 0.1% Triton X-100, and 0.1% SDS) containing cOmplete™ Mini, stored on ice for 30 minutes, and occasionally agitated. The ensuing cell lysates were transferred to fresh tubes. Supernatants and cell lysates were stored at -20°C until further use.

Protein concentration was determined with a Bradford assay (Roti®-Nanoquant #K880.1, Carl Roth, Karlsruhe, Germany) in accordance to the manufacturer's protocol. The measurement was performed on a Fluostar Omega (BMG Labtech, Ortenberg, Germany) at 590/450 nm. SDS-PAGE was performed with 40 µg protein from cell lysates and 5 µg protein from supernatant reduced in 4 x Laemmli-buffer (ROTI®Load, Carl Roth, Karlsruhe, Germany). Samples were denatured at 95°C for 5 minutes and subsequently loaded onto 4 - 15% Mini-PROTEAN® TGX™ Precast Protein Gels (Bio-Rad, Hercules, CA, USA). Gels were run at 100 V for 1 hour with western blot running buffer (25 mM TRIS Base pH 8.3, 192 mM Glycine, 0.1% SDS, pH 8.3) using the Mini-PROTEAN® Tetra Vertical Electrophoresis System (Bio-Rad, Hercules, CA, USA). Gels were blotted onto a nitrocellulose membrane (Amersham™ Protran® Premium, Sigma-Aldrich, Taufkirchen, Germany) at 100 V for 1 hour. Membranes were washed in Tris-buffered saline with Tween solution (TBST: 20 mM TRIS-HCl, pH 7.5, 150 mM NaCl, 0.1% Tween-20) and blocked with TBST containing 5% milk powder (Carl Roth, Karlsruhe, Germany) for 1 hour at room temperature. Immunostaining of GFP fusion proteins was performed with GFP Polyclonal Antibody (DyLight™ 800, Thermo Fisher Scientific, Waltham, MA, USA, 1:10,000 dilution) in cell lysate and supernatant (= growth medium) samples. GAPDH loading control monoclonal antibody (GA1R, DyLight™ 680, Thermo Fisher Scientific, Waltham, MA, USA, 1:1,000 dilution) was used for normalization of protein amount from cell lysates. Supernatants were normalized to the total protein amount using Western Blot Stain-Free Total Protein Normalization (Bio-Rad, Hercules, CA, USA). A ChemiDoc MP Imaging System (Bio-Rad Hercules, CA, USA) was

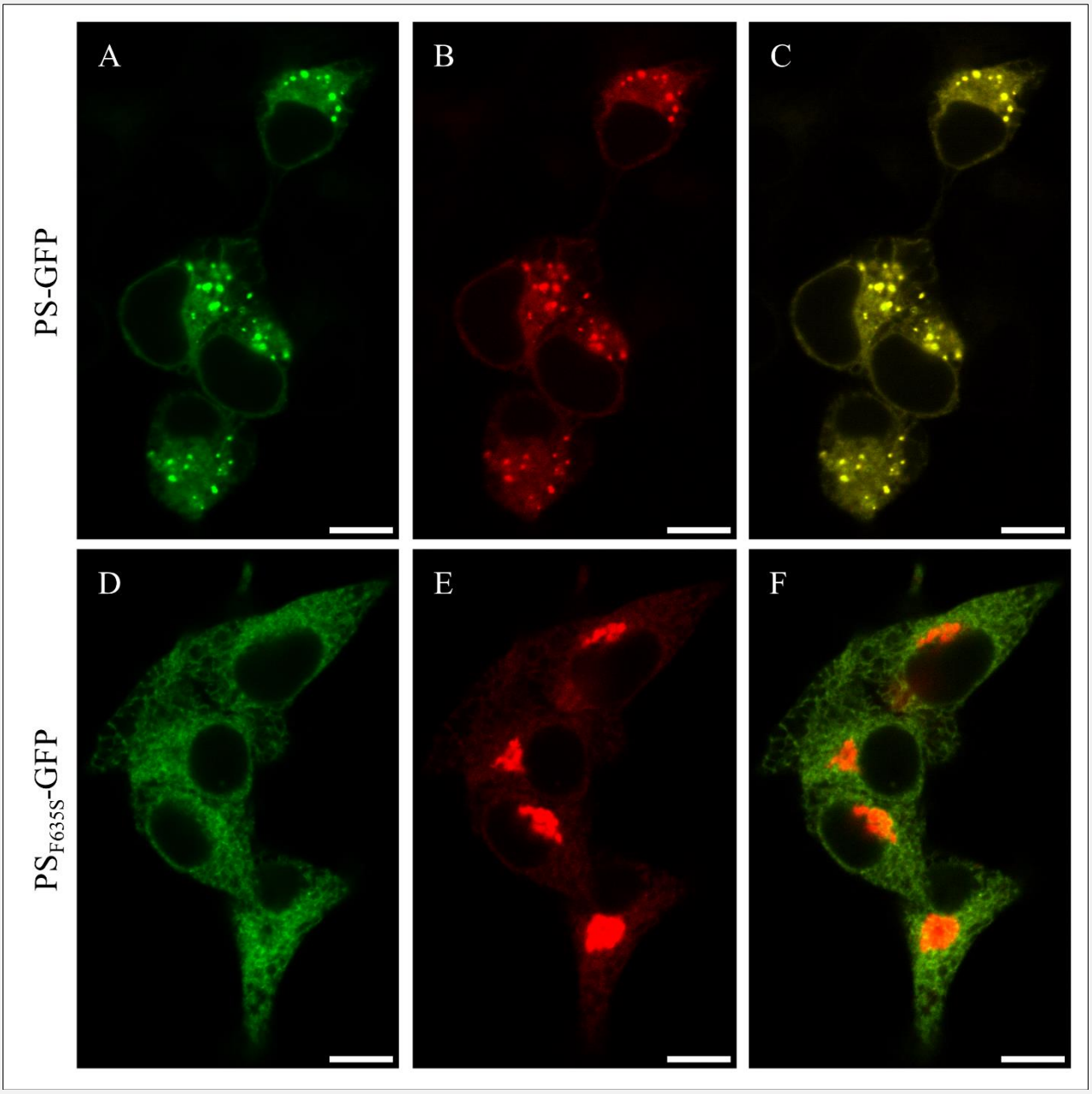

Figure 2. Subcellular localization of PS-GFP and PS$_{F635S}$-GFP in HEK293T cells.

HEK293T cells expressing constructs encoding PS-GFP (A) or PS$_{F635S}$-GFP (D) were additionally transfected with CellLight™ Golgi-RFP (B, E). PS-GFP localizes to the ER and Golgi apparatus (C), PS$_{F635S}$-GFP localizes to the ER only (F). GFP fluorescence is shown in green, RFP fluorescence in red, co-localization of GFP and RFP fluorescence is indicated in yellow. Scale bars = 10 µm.

used for imaging.

Statistical analysis

Basic statistics (mean values and standard deviations) were performed using Microsoft Excel 2016 (Office Professional Plus 2016; Microsoft, Redmond, WA, USA) and visualized using GraphPad Prism (version 9.51). Differences between cell lines were analyzed using one-way ANOVA with Bonferroni and Holm multiple comparison (all pairs simultaneously compared)

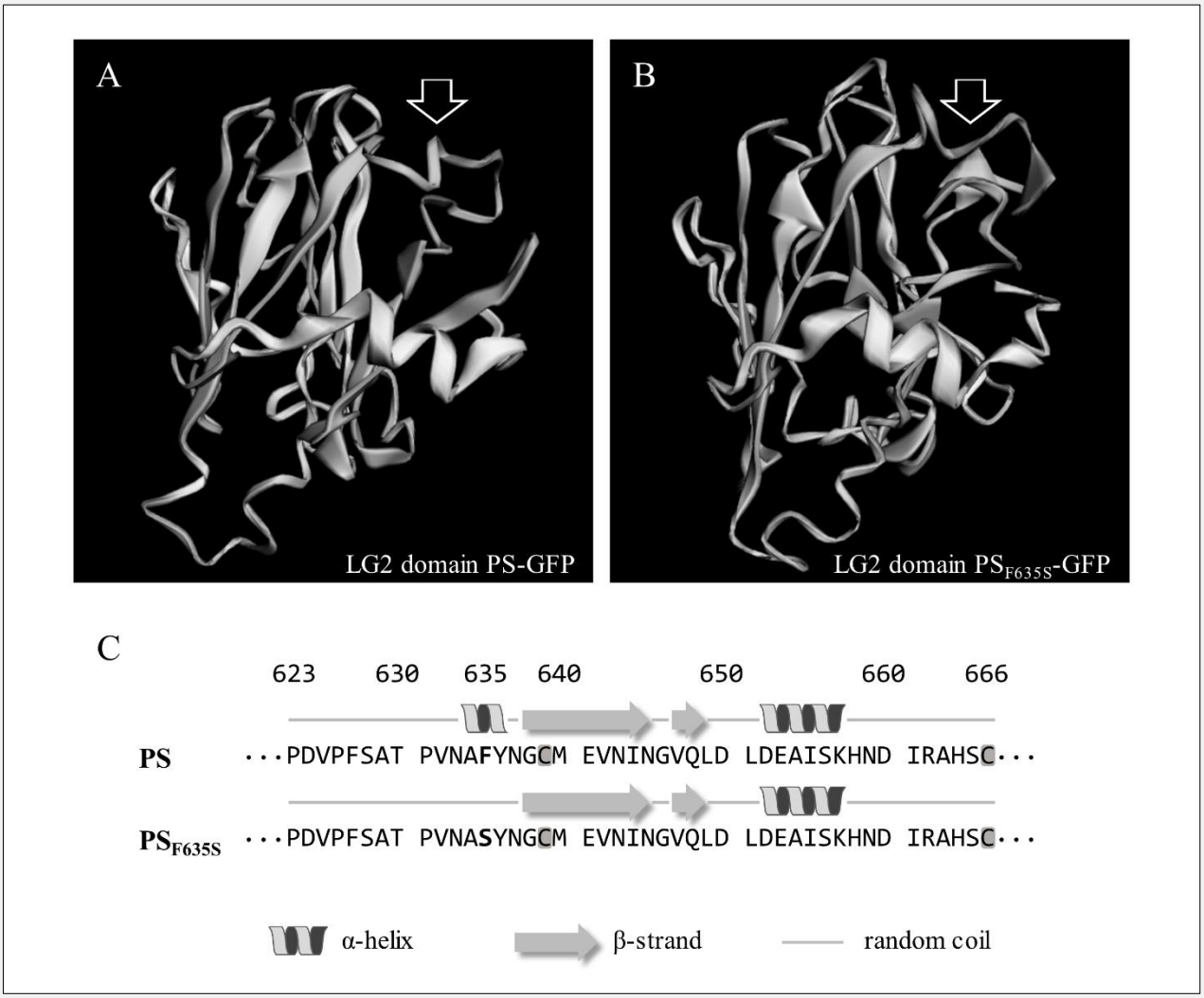

Figure 3. Predicted 3D and secondary structures for LG2 domains of native PS and PS$_{F635S}$.

Protein folding model of LG2 domains of native PS (A) and PS$_{F635S}$ (B), calculated with C-Quark [23]. (C) Secondary structure prediction according to C-Quark [23]. Amino acid exchange F635S results in deletion of a predicted α-helical structure (white arrow) that might impair formation of disulfide bond C639-C699 (cysteine residues highlighted by gray background).

(https://astatsa.com/).

Confocal microscopy

In preparation for confocal microscopy, HEK293T cell lines expressing pJR01 or pJR02 were transfected with CellLight™ Golgi-RFP, BacMam 2.0 (Life Technologies Corporation, Eugene, OR, USA) in accordance with the manufacturer`s instructions.

Images of transfected HEK293T cells were captured on a Leica TCS SP8 confocal laser scanning microscope (Leica, Wetzlar, Germany) using 488 nm (GFP) and 552 nm (RFP) laser light for excitation. GFP fluorescence was detected in a window ranging from 495 - 520 nm, RFP fluorescence in a window ranging from 570 - 595 nm. Image processing was performed with Leica Application Suite X version 2.0.1.14392 (Leica, Wetzlar, Germany).

***In silico* secondary structure prediction**

Secondary structure of PS and PS$_{F635S}$ LG2 domain (amino acids 484-666 according to UniProt entry P07 225) was predicted using the *ab initio* protein structure prediction tool C-QUARK [23].

RESULTS

HEK293T cell lines expressing *PROS1-GFP* or *PROS1*$_{c.1904T>C}$*-GFP* were established to analyze the secretion and subcellular localization of PS-GFP and PS$_{F635S}$-GFP.

HEK293T cells and growth medium of three independent cell lines per construct were analyzed by western blot for the immunolocalization of the respective GFP fusion proteins (Figure 1). PS$_{F635S}$-GFP HEK293T cells presented a trend towards higher GFP levels within the cell lumen compared to PS-GFP, but without statistical significance (Figure 1A). In contrast, PS$_{F635S}$-GFP secretion to the growth medium was significantly reduced ($p < 0.01$) for each line expressing *PROS1*$_{c.1904T>C}$*-GFP* compared to all lines expressing *PROS1-GFP* (Figure 1B).

The secretory pathway of PS-GFP and PS$_{F635S}$-GFP in HEK293T cells was visualized by detecting GFP fluorescence with a confocal laser scanning microscope (Figure 2). The Golgi apparatus was labelled using human Golgi-resident enzyme N-acetylgalactosaminyltransferase 2 (CellLight™ Golgi-RFP).

GFP fluorescence of PS-GFP, localized to the ER as well as to the Golgi apparatus (Figure 2A - C), indicates that PS-GFP is processed and secreted normally, following the secretory pathway comparable to native PS. In contrast, GFP fluorescence of PS$_{F635S}$-GFP could only be detected within the ER. No co-localization of PS$_{F635S}$-GFP and the RFP-tagged Golgi marker could be detected (Figure 2D - F).

Thus, data obtained by immunolocalization in cell lysates and cell culture supernatants as well as confocal microscopy support the hypothesis that PS$_{F635S}$ is not secreted properly, but is primarily retained within the ER.

Amino acid exchange F635S localizes to the C-terminal part of PS in the highly conserved LG2 domain [24]. A structural *in silico* prediction using C-QUARK [23] for LG2 domains of WT PS (Figure 3A) and PS$_{F635S}$ (Figure 3B) implicates that the mutation F635S disturbs an α-helical structure predicted for amino acids 634-636 (Figure 3C), thus impairing correct folding of the LG2 domain.

DISCUSSION

Secretory proteins, like PS, are synthesized into the lumen of the ER, where the initially unfolded amino acid chains mature to almost fully folded proteins (provided by chaperones and folding enzymes), before they are transported further along to the Golgi apparatus and the subsequent secretory pathway [25,26]. An inevitable precondition for the secretory pathway is the passing of the ER quality control [27,28]. Misfolded proteins that fail to comply with ER quality control undergo ER-associated protein degradation [27]. The observed accumulation of PS$_{F635S}$-GFP within the ER, without further transport to the Golgi apparatus (Figure 2) and an accordingly strongly reduced secretion (Figure 1) is in line with an incorrect folding of PS$_{F635S}$. This is confirmed by *in silico* modeling of the mutated PS LG2 domain, where amino acid exchange F635S results in loss of an α-helical structure and a subsequently altered conformation of the LG2 domain (Figure 3).

Protein databases Swiss-Modell (https://swissmodel.expasy.org/) and UniProt (https://www.uniprot.org/) predict a disulfide bond in the LG2 domain of WT PS between C639 and C666, with C639 in proximity to F635, which is mutated to S in PS$_{F635S}$.

Disulfide bonds in secretory proteins are mostly formed during the folding process in the ER lumen [29]. Two different forming mechanisms are postulated for disulfide bonds, with most proteins being folded by following a hybrid of both model mechanisms [29]: the structured precursor mechanism, in which a structured, native-like folded intermediate exists before disulfide bond formation takes place [30] and a quasi-stochastic mechanism, in which disulfide bonds are formed before conformational folding [31]. It seems likely that mutation F635S might impair the formation of disulfide bond C639-C699. The exchange of the bulky hydrophobic side chain of F against the short polar side chain of S results in a (predicted) structural change from α-helical to random coil (Figure 3C). Thus, this mutation might impair a structured pre-folding required for disulfide bonding according to the structured precursor mechanism or abolish the required proximity of C639 and C699 for formation of a disulfide bond for the quasi-stochastic mechanism [29,31]. Whether mutation F635S, in fact, affects protein folding in such a way that disulfide bond C639-C699 can no longer be formed remains a matter of speculation. Nevertheless, the data presented clearly show that PS folding is impaired by mutation F635S to such an extent that a proper secretion is no longer feasible. Here, an additional point to address is whether the folding of complete PS protein is altered or only altered in the LG2 domain. As folding occurs subsequent to secretion into the ER lumen [28], with F635S being a very C-terminal mutation, and as the SHBG domain (consisting of LG1 and LG2) can fold independently of other domains [32], it seems likely that correct folding of only the LG2 domain is impaired.

As postulated recently [1], a secretion defect due to the single amino acid exchange F635S in the LG2 domain, comparable to what has been described for several variants in close proximity to F635 [10,12,18-20], could be confirmed with the data presented here. Thus, the PS Erlangen mutation results in type I PS deficiency caused by a secretion defect.

Acknowledgment:
We thank all patients and donors for providing blood at the Clinical Department of Transfusion Medicine and Hemostaseology in Erlangen and all colleagues involved for supporting this study. The present work was

performed in fulfillment of the requirements for obtaining the degree “Dr. med.” for Julian Reißig.

Source of Funds:
We acknowledge financial support by the Deutsche Forschungsgemeinschaft and Friedrich-Alexander-University Erlangen-Nürnberg (FAU) within the funding program “Open Access Publication Funding”.

Declaration of Interest:
There are no conflicts of interest for any of the listed authors.

References:

1. Schneider S, Reißig J, Weisbach V, Achenbach S, Strobel J, Hackstein H. Protein S Erlangen: a novel *PROS1* gene mutation associated with quantitative protein S deficiency. Blood Coagul Fibrinolysis 2022;33(4):224-7. (PMID: 34939974)

2. Esmon CT. The regulation of natural anticoagulant pathways. Science 1987;235(4794):1348-52. (PMID: 3029867)

3. Dahlback B. Blood coagulation. Lancet 2000;355(9215):1627-32. (PMID: 10821379)

4. Griffin JH, Zlokovic BV, Mosnier LO. Protein C anticoagulant and cytoprotective pathways. Int J Hematol 2012;95(4):333-45. (PMID: 22477541)

5. Dahlback B, Stenflo J. High molecular weight complex in human plasma between vitamin K-dependent protein S and complement component C4b-binding protein. Proc Natl Acad Sci USA 1981; 78(4):2512-6. (PMID: 6454142)

6. Toledano-Sanz P, Reventun P, Viskadourou M, et al. The transcriptional landscape of human liver endothelial cells. Blood Adv 2023;7(10):2047-52. (PMID: 36634263)

7. Gandrille S, Borgel D, Sala N, et al. Protein S deficiency: a database of mutations-summary of the first update. Thromb Haemost 2000;84(11):918. (PMID: 11127877)

8. Pintao MC, Garcia AA, Borgel D, et al. Gross deletions/duplications in *PROS1* are relatively common in point mutation-negative hereditary protein S deficiency. Hum Genet 2009;126(3):449-56. (PMID: 19466456)

9. Espinosa-Parrilla Y, Morell M, Souto JC, et al. Protein S gene analysis reveals the presence of a cosegregating mutation in most pedigrees with type I but not type III PS deficiency. Hum Mutat 1999;14(1):30-9. (PMID: 10447256)

10. Biguzzi E, Razzari C, Lane DA, et al. Molecular diversity and thrombotic risk in protein S deficiency: the PROSIT study. Hum Mutat 2005;25(3):259-69. (PMID: 15712227)

11. Ten Kate MK, Platteel M, Mulder R, et al. *PROS1* analysis in 87 pedigrees with hereditary protein S deficiency demonstrates striking genotype-phenotype associations. Hum Mutat 2008;29(7): 939-47. (PMID: 18435454)

12. Hurtado B, Munoz X, Mulero MC, et al. Functional characterization of twelve natural *PROS1* mutations associated with anticoagulant protein S deficiency. Haematologica 2008;93(4):574-80. (PMID: 18322254)

13. Taniguchi F, Morishita E, Sekiya A, et al. Gene analysis of six cases of congenital protein S deficiency and functional analysis of protein S mutations (A139V, C449F, R451Q, C475F, A525V and D599TfsTer13). Thromb Res 2017;151:8-16. (PMID: 28088608)

14. Beauchamp NJ, Daly ME, Makris M, Preston FE, Peake IR. A novel mutation in intron K of the PROS1 gene causes aberrant RNA splicing and is a common cause of protein S deficiency in a UK thrombophilia cohort. Thromb Haemost 1998;79(06):1086-91. (PMID: 9657428)

15. Tatewaki H, Iida H, Nakahara M, et al. A novel splice acceptor site mutation which produces multiple splicing abnormalities resulting in protein S deficiency type I. Thromb Haemost 1999; 82(1):65-71. (PMID: 10456456)

16. Mizukami K, Nakabayashi T, Naitoh S, et al. One novel and one recurrent mutation in the PROS1 gene cause type I protein S deficiency in patients with pulmonary embolism associated with deep vein thrombosis. Am J Hematol 2006;81(10):787-97. (PMID: 16868938)

17. Zhang YP, Lin B, Ji YY, et al. A thrombophilia family with protein S deficiency due to protein translation disorders caused by a Leu607Ser heterozygous mutation in *PROS1*. Thromb J 2021; 19(1):64. (PMID: 34496879)

18. Espinosa-Parrilla Y, Yamazaki T, Sala N, Dahlback B, de Frutos PG. Protein S secretion differences of missense mutants account for phenotypic heterogeneity. Blood 2000;95(1):173-9. (PMID: 10607700)

19. Tsuda H, Urata M, Tsuda T, et al. Four missense mutations identified in the protein S gene of thrombosis patients with protein S deficiency: effects on secretion and anticoagulant activity of protein S. Thromb Res 2002;105(3):233-9. (PMID: 11927129)

20. Li M, Long GL. Identification of two novel point mutations in the human protein S gene associated with familial protein S deficiency and thrombosis. Arterioscler Thromb Vasc Biol 1996;16(12): 1407-15. (PMID: 8977443)

21. Gibson DG, Young L, Chuang RY, Vente JC, Hutchison CA 3rd, Smith HO. Enzymatic assembly of DNA molecules up to several hundred kilobases. Nat Methods 2009;6(5):343-5. (PMID: 19363495)

22. Zheng L, Baumann U, Reymond, JL. An efficient one-step site-directed and site-saturation mutagenesis protocol. Nucleic Acids Res 2004;32(14):e115. (PMID: 15304544)

23. Mortuza SM, Zheng W, Zhang C, Li Y, Pearce R, Zhang Y. Improving fragment-based ab initio protein structure assembly using low-accuracy contact-map predictions. Nat Commun 2021;12: 5011. (PMID: 34408149)

24. García de Frutos P, Fuentes-Prior P, Hurtado B, Sala N. Molecular basis of protein S deficiency. Thromb Haemost 2007;98(3): 543-56. (PMID: 17849042)

25. Kuznetsov G, Nigam SK. Folding of secretory and membrane proteins. N Engl J Med 1998;339(23):1688-95. (PMID: 9834307)

26. Sicari D, Igbaria A, Chevet E. Control of protein homeostasis in the early secretory pathway: current status and challenges. Cells 2019;8(11):1347. (PMID: 31671908)

27. Anelli T, Sitia R. Protein quality control in the early secretory pathway. EMBO J 2008;27(2):315-27. (PMID: 18216874)

28. Robinson PJ, Bulleid NJ. Mechanisms of disulfide bond formation in nascent polypeptides entering the secretory pathway. Cells 2020;9(9):1994. (PMID: 32872499)

29. Welker E, Wedemeyer WJ, Narayan M, Scheraga HA. Coupling of conformational folding and disulfide-bond reactions in oxidative folding of proteins. Biochemistry 2001;40(31):9059-64. (PMID: 11478871)

30. Feige MJ, Braakman I, Hendershot LM. CHAPTER 1.1 Disulfide Bonds in Protein Folding and Stability. In Oxidative Folding of Proteins: Basic Principles, Cellular Regulation and Engineering; The Royal Society of Chemistry: London, UK, 2018; 1-33. https://books.rsc.org/books/edited-volume/711/chapter/418161/Disulfide-Bonds-in-Protein-Folding-and-Stability

31. Camacho CJ, Thirumalai D. Modeling the role of disulfide bonds in protein folding: Entropic barriers and pathways. Proteins 1995; 22(1):27-40. (PMID: 7675784)

32. Saposnik B, Borgel D, Aiach M, Gandrille S. Functional properties of the sex-hormone-binding globulin (SHBG)-like domain of the anticoagulant protein S. Eur J Biochem 2003;270(3):545-55. (PMID: 12542704)